



DOI: 10.34910/MCE.105.14

## Thin-walled compressed steel constructions under fire load

M.V. Gravit<sup>a</sup> , I.I. Dmitriev<sup>\*b</sup> 

<sup>a</sup> Peter the Great St. Petersburg Polytechnic University, St. Petersburg, Russia

<sup>b</sup> Graz University of Technology, Graz, Austria

\*E-mail: [i.i.dmitriev@yandex.ru](mailto:i.i.dmitriev@yandex.ru)

**Keywords:** steel construction, thin walled structures, cold-formed steel, structural design, fire, fire safety, fire protection, fire design

**Abstract.** The article demonstrates the both theoretical and actual fire resistance limits of the composite I-shaped and box-shaped thin-walled steel structures in compression conditions under the standard fire load. The calculation was based on the Eurocode 3 and finite element modeling of high-temperature fields in SOFiSTiK PC. The experimental tests were carried out on the basis of design data to validate the results of both the calculation and modeling. It is shown that the static part of the calculation of the critical temperature, upon irreversible plastic deformations occur, is solved not completely correctly by means of regulations. In average the calculated critical temperature exceeds the actual one on 50-80 °C. It is shown that the assumption of a critical temperature equals to 350 °C is unreasonably low. The complex graphs of the temperature growth for each steel construction are given according to the paragraphs of normative documents, the finite-element modeling and results of thermocouple indicators for the fire tests. The solution of thermophysical part of calculation according to Eurocode 3 showed good convergence with the results of the experimental data, including the samples with effective fire protection, but strongly depend on the step of calculation. The accurate results were reached only when the time step equals 1 sec. The finite element modeling predicted the correct time to achieve the critical temperature of the tested sample without any additional assumptions. The MBOR-16F material produced by TIZOL JSC was used as a flame protection. This is new material, which has not been previously studied yet. The recommendations on application of the finite element programs are given in the thermophysical part of the fire resistance calculation.

### 1. Introduction

Bearing and enclosing structures based on the thin-walled galvanized steel profiles are rapidly spreading in construction area. The light gauge steel framing (LGSF or LSF) is widely used in low-rise constructions because of the wide architectural capabilities and excellent technical and economical qualities that allow operating in dynamic conditions of a changing market with maximum accuracy, flexibility and efficiency.

The classical formulas of structural mechanics and theory of elasticity are commonly used in the calculation of steel sections, however taking into account specificity of thin-walled elements such as reduction of the area for some elements under the load or particular work outside of elastic deformation zone.

The LGSF constructions have great perspectives in the construction area [1, 2], but low level of fire resistance and also insufficient research on both unprotected and different types of fire-protective materials for various structures inhibit their implementation. The fire resistance of thin-walled rods is actively discussed throughout the world but despite the numerous investigations of these structures, this issue has not been fully studied and remains relevant nowadays.



The majority of studies connected with the given designs have theoretical character and some experimental data on strength characteristics (including those connected with issues of local and general stability, resistance to compression, bending, torsion in the whole profile and its elements) only at room temperatures [2–7].

It is necessary to pay more attention to measures for maintaining fire safety and ensuring the standard fire resistance of all structures, especially in case of designing metal frame buildings and structures [8, 9]. This problem is extremely relevant for thin-walled structures due to the high thermal conductivity of steel and the small value of the reduced thickness of the cross-section. Rapid temperature rise in the thin-wall cross section will lead to sharp deterioration of mechanical characteristics.

There is a limited number of works devoted to studying the behavior of thin-walled structures under the influence of high temperatures. There are some studies, which show the influence of the value of the limiting deviation of geometric dimensions [10] or influence on the load-bearing capacity by the value of imperfection of structures [11]. Nowadays, EN1993-1.2 [12] does not include a simplified method for calculating of thin-walled structures, but only offers recommendations for cold-formed sections (class 4) to take the critical heating temperature as 350 °C.

The results of this work, as well as examples of similar studies [13–18], show these values to be unreasonably low. For example, under certain boundary conditions, columns and beams (especially composite ones) made of high-strength steel can retain their bearing capacity at temperatures up to 700 °C.

There is a small number of works concerning the fire resistance of LSF, which includes consideration of the regulatory framework, modelling and experimental studies of authors such as N.I. Vatin, M.R. Garifullin [19–21], M.V. Gravit [22, 23], M.Z. Naser [24, 25], W. Chen, J. Ye [26–30], Y. Dias [31, 32]. Only few studies have investigated the behavior of thin-walled steel structures under the fire load, but most of them came to the conclusion that cold-formed steel constructions have higher fire resistance than the Eurocode 3 limit of 350 °C.

The aim of the article is to substantiate the fire resistance limit of composite I-shaped and box-shaped thin-walled steel structures under compression conditions under standard fire load in cases of absence and presence of the effective fire protection.

To achieve this goal, the following tasks are solved:

- 1) Analytical calculation of the structure on the basis of Eurocode 3;
- 2) Finite-element modeling of the high-temperature fields for each complex cross-section in SOFiSTiK PC;
- 3) Fire tests based on theoretical calculation;
- 4) Deviation analysis of both analytical and finite element calculations with thermocouple results in experimental tests.

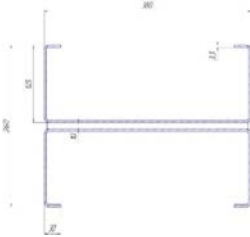
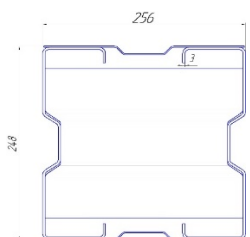
Profiles were tested under load. Two cross-sections were considered as the tested samples (Table 1):

1. I-shaped section consists of two C-shaped profiles 380×125×30×3.5 connected through a flange 10 mm by bolt fastening.
2. Box-shaped section consists of two  $\Sigma$ -shaped profiles 245×80×20×3 connected through a flange 1.5 mm by bolt fastening.

Profiles were tested both without fire protection and with the use of special flame-protection roll material MBOR-16F produced by TIZOL JSC.

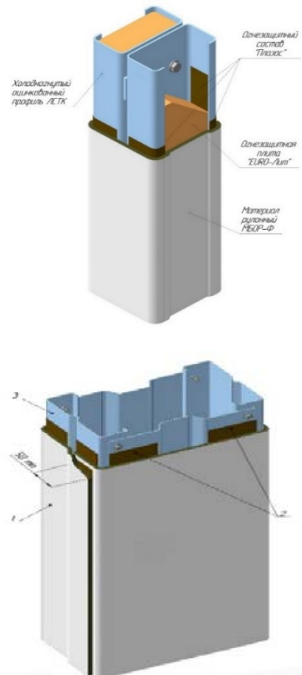
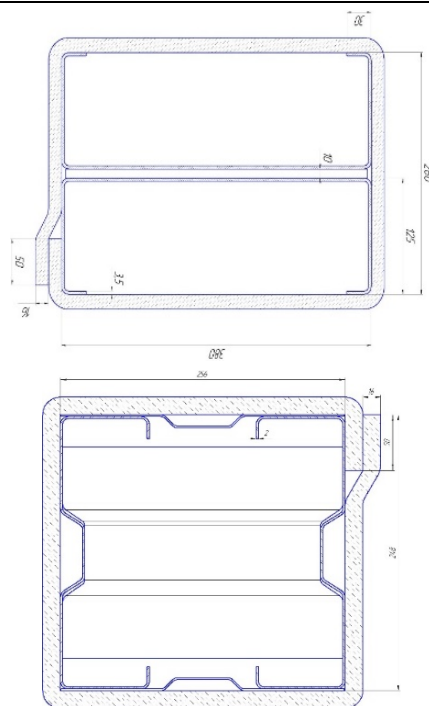
The effective characteristics of the profiles in compression conditions are presented in Table 1.

**Table 1. Calculation characteristics of the composite structures.**

Scheme	Characteristics
	$A_g^I = 2 \cdot 2310.63 = 4621.26 \text{ mm}^2 = 46.21 \text{ cm}^2$ $A_{eff}^I = 2 \cdot 1251.77 = 2503.54 \text{ mm}^2 = 25.04 \text{ cm}^2$ $I_{eff}^I = 1433.72 \text{ cm}^4$ <p>Length <math>l = 3000 \text{ mm}</math>            Static load is equal <math>E_{fi,d} = 31.0 \text{ t}</math></p>
	$A_g^I = 2 \cdot 1295.77 = 2591.54 \text{ mm}^2 = 25.92 \text{ cm}^2$ $A_{eff}^I = 2 \cdot 1212.75 = 2425.50 \text{ mm}^2 = 24.26 \text{ cm}^2$ $I_{eff}^I = 2889.28 \text{ cm}^4$ <p>Length <math>l = 3000 \text{ mm}</math>            Static load is equal <math>E_{fi,d} = 15.1 \text{ t}</math></p>

To simplify the calculation scheme of the column with fire protection material produced by TIZOL JSC as well as in accordance with the program of fire tests, the additional fireproof plate "Euro-Lit" and fireproof composition is excluded from the calculation. The critical temperature was calculated using the full analytical calculation method according to the EuroCode [12].

**Table 2. The solution of the column fire protection produced by TIZOL JSC and the calculation scheme of the composite section.**

Picture	Scheme
	

The scientific novelty of this study is the choice of composite cross-section profiles (rather than simple C-shaped profiles) as the object to be tested, which are usually used as supporting structures in buildings and structures. A new effective fire protection roll material MBOR-16F was used as fire protection.

## 2. Method

### 2.1. Analytical calculation

The basic principle of calculation for the steel structures on the fire resistance is to provide necessary and sufficient durability (bearing capacity) throughout the required time period. The most common analytical method is to determine the critical heating temperature of a structure for a given load. The material temperature  $\theta_d$  during the fire load have to be less (or equal) to the design critical material temperature.

$$\theta_d < \theta_{cr,d} \quad (1)$$

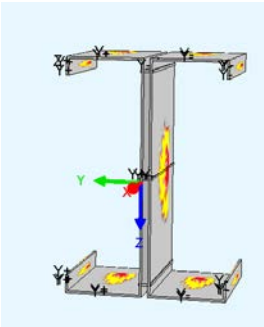
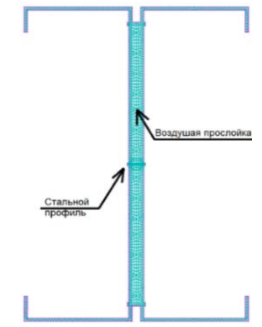
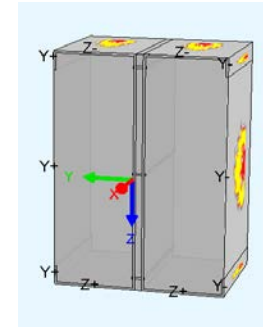
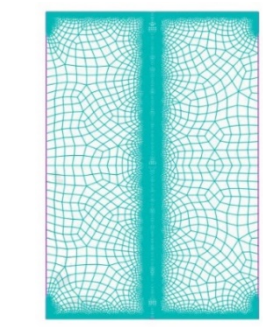
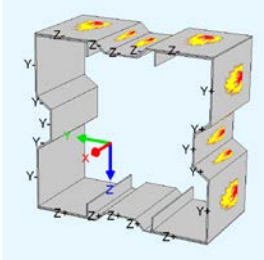
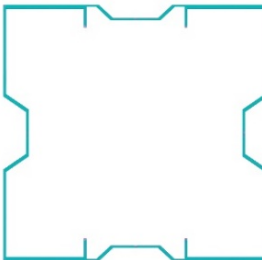
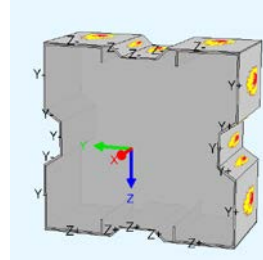
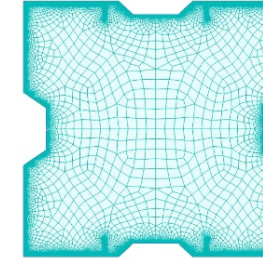
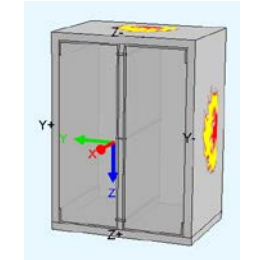

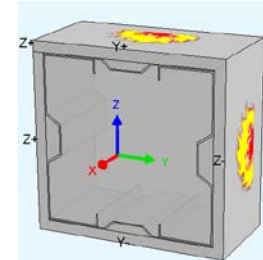
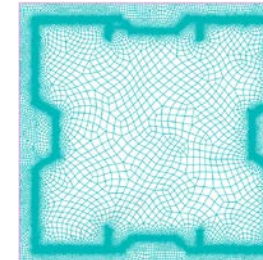
Based on this thesis, the strength calculation determines the reduced bearing capacity after the necessary time. A comparison on time parameters is used to determine the need of the fire protection for each element.

### 2.2. Modelling

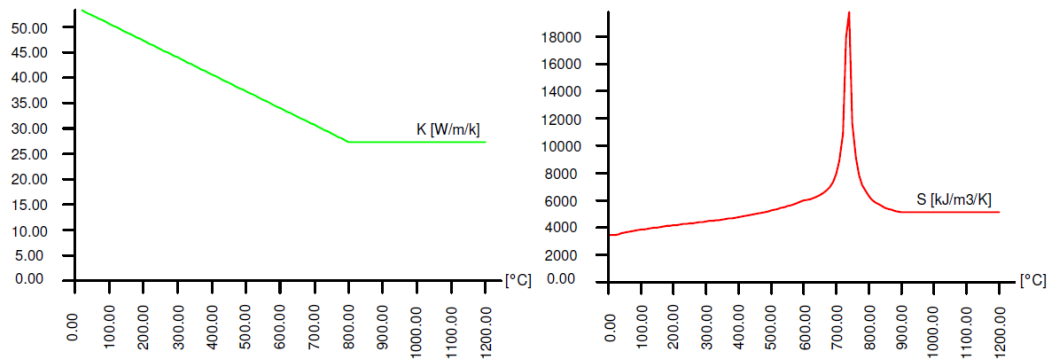
All calculations of a structure are carried out by a method of finite elements on the basis of spatial model. The section elements used for calculation of a steel rod construction are given in Table 3. The Hydra module of the SOFiSTiK software package (ver. 2020) was used for the analysis of temperature distribution over the cross-section of the considered structure. Data input was made using the internal instrumental programming language CADINP in the text editor Teddy. Boundary conditions of the considered models correspond to boundary conditions of the experimental program (temperature is equal to 20 °C, thermal resistance is equal to 9.000 W/K/m<sup>2</sup>). The grid is quadrangular. Cell size is not constant with higher density in the area of material and model boundaries. Grid resolution is equal at least 0.01 m.

In sections without fire protection two alternative models with and without air gap were considered.

**Table 3. Calculated finite element models.**

N	Calculated scheme and finite element models			
1				
2				
3				

The properties and geometric dimensions of the structures are set in accordance with the real properties of materials and the samples' overall dimensions. Thermal characteristics of materials specified in the design model. Thermal Conductivity and Heat Capacity of steel are presented in Fig. 1. Numerical dependencies of fire protection are given as equation (2, 3).



**Figure 1. Thermal Conductivity and Heat Capacity of Structural Steel.**

Thermal properties of fire protection:

Specific heat capacity  $c_p$  of fire protection in dependence of the temperature  $\theta_p$  (°C):

$$c_p = 582 + 0.63(\theta_p + 273) = 754 + 0.63 \cdot \theta_p \frac{\text{J}}{\text{kg} \cdot \text{K}} \quad (2)$$

Thermal conductivity  $\lambda_p$  of fire protection in dependence of the temperature  $\theta_p$  (°C) based on an analysis of the manufacturer's data:

$$\lambda_p = 0.0284 + 0.0002 \cdot \theta_a \frac{\text{W}}{\text{m} \cdot \text{K}} \quad (3)$$

$$\text{Density of fire protection } \rho_p = 100 \frac{\text{kg}}{\text{m}^3}.$$

The system is uniformly heated by the external heat flow; all energy is used to increase the system temperature taking into account its heat capacity. The heating process stops when the temperature at the external boundaries is equalized with the temperature of the external irradiating medium, which corresponds to the standard fire mode and the set temperature in the furnace.

### 2.3. Fire test

The furnace for fire tests in the Tizol JSC laboratory is a fire chamber lined with fireclay bricks with a loading device for creating compressive forces in the cross-section of the structure and a mechanism for fixation and support. The chrome-aluminum thermocouples were used in the middle section of the structure for the I-beam type and between the profile and the connecting plate for the box type to measure the temperature. The general view of the fire-testing machine in the Fig. 2. The thermocouples of I-shaped construction are located in the center between of C-shaped profiles. The thermocouples of box-shaped sections are in between of steel plates.



**Figure 2. Test furnace.**

The test method consists of determining the time of the limit state of load-bearing capacity (R) due to caving or critical deformation. The fixed time will be considered the actual fire resistance limit of the structure under test. The R limit state according to the Russian government standard GOST 30247.1-94



comes when vertical deformation reaches one hundredth of the length of the structure, which in our case is 30 mm. The standard fire mode according to the Russian government standard GOST 30247.0-94 and international standard ISO 834 was considered:

$$\theta_g = 20 + 345 \lg(8t + 1) \quad (4)$$

$t$  is time, min;

$\theta_g$  is temperature inside the furnace  $t$ , °C.

### 3. Results and Discussion

#### 3.1. The samples without fire protection

##### 3.1.1. Static part of calculation

The bearing capacity of the steel structure is assumed to be preserved after the time  $t$  for the specified fire mode when the condition is fulfilled:

$$E_{fi,d} < R_{fi,d} \quad (5)$$

$R_{fi,d}$  is calculated value of the fire resistance at the moment of time  $t = 0$ .

The calculation is performed taking into account the yield strength analysis for cross sections Class 4 and the effective cross-sectional area of the thin-walled structure. The results are given in according to the static load for each cross-section (Table 1). The critical temperature is a linear interpolation between the calculated load-carrying capacity and actual one [12]. The critical temperature is equal to:

1<sup>st</sup> sample:  $\theta_{cr} = 547.27$  °C (static load is 31.0  $t$ );

2<sup>nd</sup> sample:  $\theta_{cr} = 713.08$  °C (static load is 15.1  $t$ ).

##### 3.1.2. Thermophysical part of calculation

###### 3.1.2.1. Analytical solution

The load-bearing capacity is considered exhausted when the material of construction reaches the temperature  $\theta_d$  with value higher than the critical temperature. The calculation is performed for temperatures with a time interpolation step not exceeding the recommended value until the structure reaches the critical temperature. The temperature growth delta is determined on the basis of the absorbed heat flow taking into account the convection and radiant heat exchange as well as the thermophysical properties of materials.

$$\Delta\theta_{a,t} = k_{sh} \cdot \frac{A_m}{Vc_a\rho_a} \dot{h}_{net} \Delta t$$

The results of the thermophysical calculation by the analytical method are given in the graphical form on the final graph (Fig. 5) at the end of the section. The results depends on the time step and the most accurate results were reached only with the time step equals to 1 sec.

###### 3.1.2.2. Finite element solution with the SOFiSTiK PC (ver. 2020)

The value in the center of the section for the I-shaped and between the steel plates for the box-shaped section was taken as the design temperature.

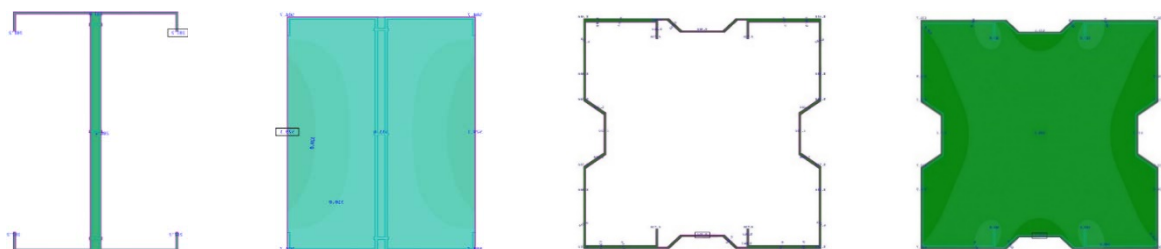


Figure 3. Simulated cross-sections of the samples.


The modeling results are graphs with temperature gradient over the cross-section (Fig. 3). Modeling results for the I-beam section show a significant difference between the sample with and without air gap.

For the box section the accounting of the internal air did not effect on the temperature gradient in the steel parts of the structure.

### 3.1.3. Fire test

Together with Tizol JSC, fire tests of the unprotected profiles were conducted. There are some photos of the tested samples and a diagram of temperature rise in field tests (Table 4). The tested samples are installed in the furnace chamber arranged according to the Russian government standard GOST 30247.1-94. The load is set at least 30 minutes before the start of the test and is maintained (with an accuracy of +/- 5 %) constant throughout the test. Static load for the 1<sup>st</sup> sample is equal to 31.0 t and for the 2<sup>nd</sup> sample is equal to 15.1 t.

**Table 4. Test samples during the fire load.**

No	Test samples		
1			
2			

Critical deformations of the first specimen were observed at 9 minutes 33 seconds of testing. The maximum average temperature of the specimen is 451.3 °C. For the second specimen, the critical temperature is 649.9 °C and the time to reach the limit state is 12 minutes 10 seconds respectively. The temperature changes of the furnace thermocouples and the specimen are shown in Fig. 4.



**Figure 4: Graphic of temperature changes at thermocouples (monitor of test equipment TIZOL JSC):**  
 Red – upper limit of temperature deviation tolerance from ISO curve;  
 Blue (dark) – lower limit of temperature deviation tolerance from ISO curve;  
 Green – set temperature in the furnace;  
 Black – actual average temperature in the furnace;  
 Blue – average sample heating temperature.

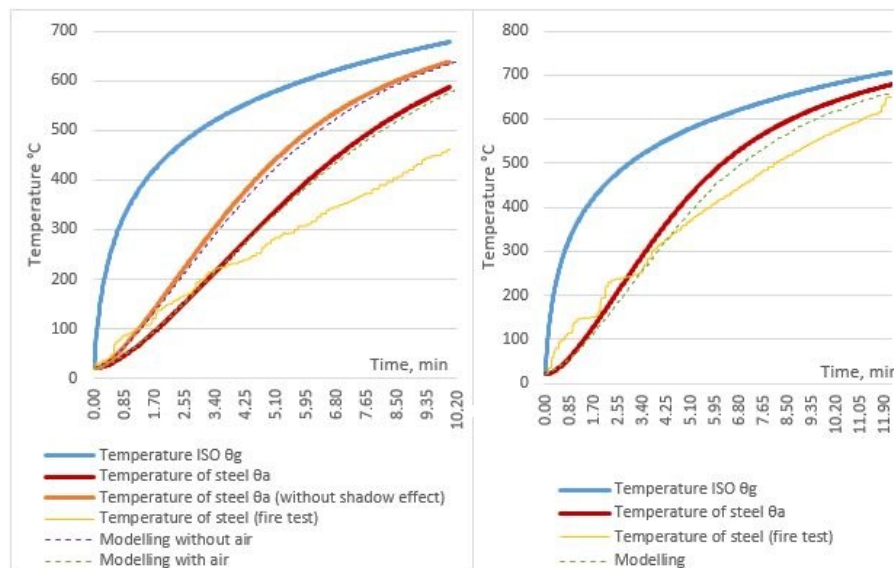
The accuracy of experimental results is ensured by the sufficient number of thermocouples and the experimental error does not exceed 10 %.

A summary of results of the static, thermophysical calculations and the results of fire tests are presented in Table 5.

**Table 5. Summary data on critical temperatures and fire resistance limits for unprotected samples.**

Calculation method	Sample 1		Sample 2	
	Calculation	Fire test	Calculation	Fire test
Static calculations				
Critical temperatures °C	547.27	451.3°C	713.08°C	649.9°C
Thermophysical calculations. Fire resistance limits, min (min)				
Analytical solution	8.942		14.790	
Simulation (including air gap)	9.231		15.150	
Calculation with $k_{sh} = 1$ (without shadow effect)	7.055	09:33	–	12:10
Simulation (without air gap)	7.440		15.150	

The calculated fire exposure curves and actual thermocouple values are shown in Fig. 5.



**Figure 5. Fire exposure curves (calculated and actual) for unprotected samples.**

Finite element modeling has shown excellent convergence with the results of calculations according to European standard EN 1993-1-2. In the case of the I-shaped section, the air gap modeling showed compliance with the curve, which calculation included shading factor, and without air for a conservative solution (without shade effect). The actual high-temperature curve obtained during the fire tests are mostly below than calculated values due to additional convective effects realized in the present tests in the fire chamber, imperfection of thermocouples and other external independent factors, which cannot be completely excluded from the experiment data. In general, the convergence between the calculated and actual curves for the first (I-shaped) sample can be considered satisfactory, and for the second (box-shaped) sample good.

### 3.2. The samples with fire protection

#### 3.2.1. Thermophysical part of calculation

##### 3.2.1.1. Analytical solution

The area  $A_p$  of fire protective material is taken as the area of its inner surface. In case of uniform temperature distribution in the cross-section of the steel protected structure, the temperature increase  $\Delta\theta_{a,t}$  for the period of time  $\Delta t$  is determined from the following expression (§4.2.5.2, EN 1993-1-2):



$$\Delta\theta_{a,t} = \frac{A_p \lambda_p}{V d_p} \cdot \frac{(\theta_{g,t} - \theta_{a,t})}{c_a \rho_a (1 + \frac{\varphi}{3})} \cdot \Delta t - (e^{\frac{\varphi}{10}} - 1) \cdot \Delta\theta_{g,t} \text{ where } \varphi = \frac{c_p \rho_p}{c_a \rho_a} d_p \frac{A_p}{V}$$

$A_p$  is inner surface area of the fire protection material per unit of construction length (m<sup>2</sup>/m);

$V$  is volume of the unit of construction length (m<sup>3</sup>/m);

$c_a$  is specific heat capacity of steel depending on temperature (J/(kg K));

$c_p$  is specific heat capacity of fire protective material independent of temperature (J/(kg K));

$d_p$  is thickness of the fire protection (m);

$\Delta t$  is time interval (s), not exceeding 30 s;

$\theta_{a,t}$  is steel temperature at time  $t$  (°C);

$\theta_{g,t}$  is ambient gas temperature at time  $t$  (°C);

$\Delta\theta_{g,t}$  is ambient gas temperature increase during the time period  $\Delta t$  (K);

$\lambda_p$  is thermal conductivity of the fire protection system (W/(m K));

$\rho_a$  is steel density (kg/m<sup>3</sup>);

$\rho_p$  is fire protective material density (kg/m<sup>3</sup>).

The Eurocode prescribes to take the specific heat capacity of the fire protective material independent of the temperature. The thermal conductivity varies depend on the temperature of fire protection. The results depends on the iteration step and the most accurate results were reached only with the time step equals to  $\Delta t = 1$  sec. The solution of the thermophysical problem by the analytical method is given in graphical form on the final graph at the end of the section.

3.2.1.2. Finite element solution with the SOFiSTiK PC (ver. 2020)

The value in the center of the section was taken as the design temperature. The simulation results are graphs with a temperature gradient across the section (Fig. 6). The internal filling of the profile is air.

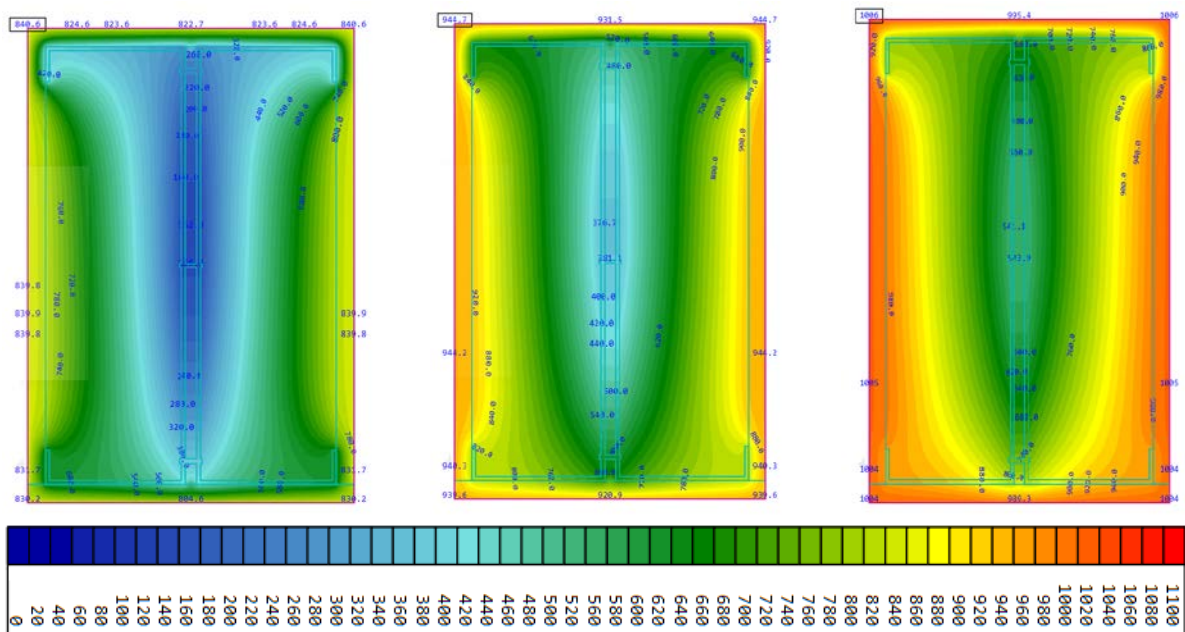


Figure 6. Temperature gradient at 30, 60 and 90 minutes.

Similarly, the fire resistance limit was calculated for the box-shaped section. Calculation point is located between steel plates (Fig. 7).

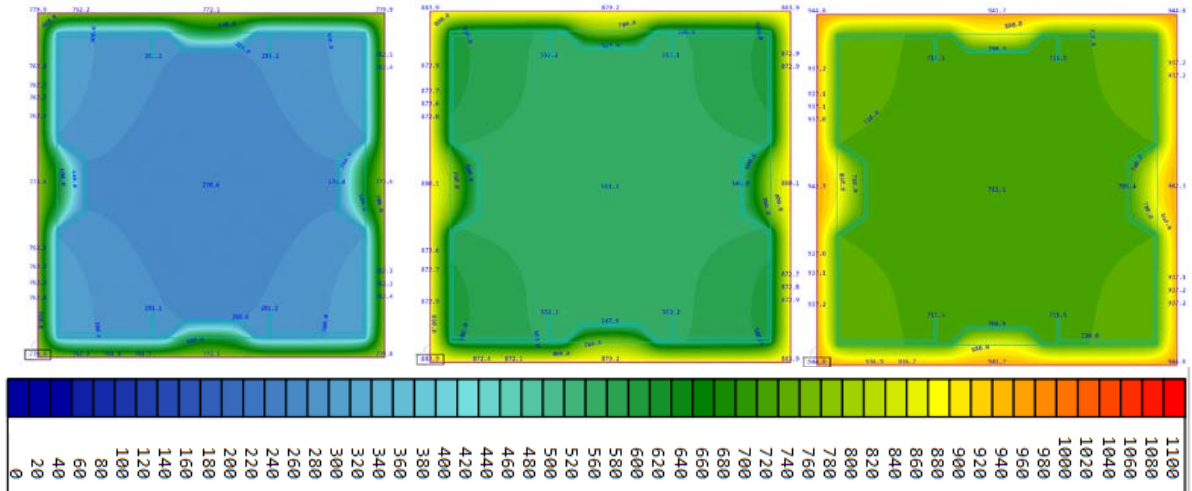


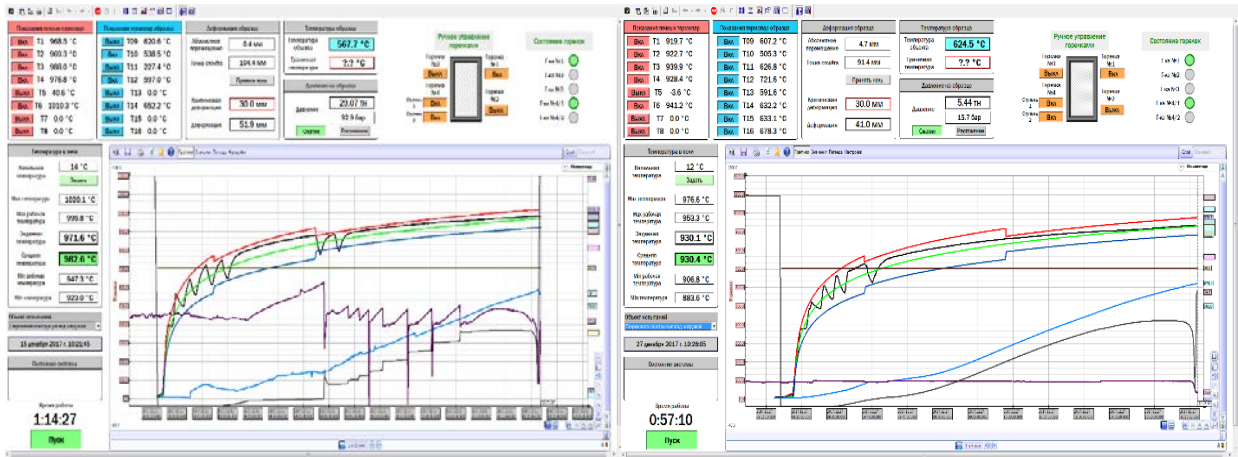
Figure 7. Temperature gradient at 20, 40 and 60 minutes.

### 3.2.2. Fire test

Together with Tizol JSC, fire tests of the profiles with effective fire protection MBOR-16F were conducted. Below you can see photos of the tested samples and a diagram of temperature rise in field tests.

Table 6. Test samples before and during fire test.

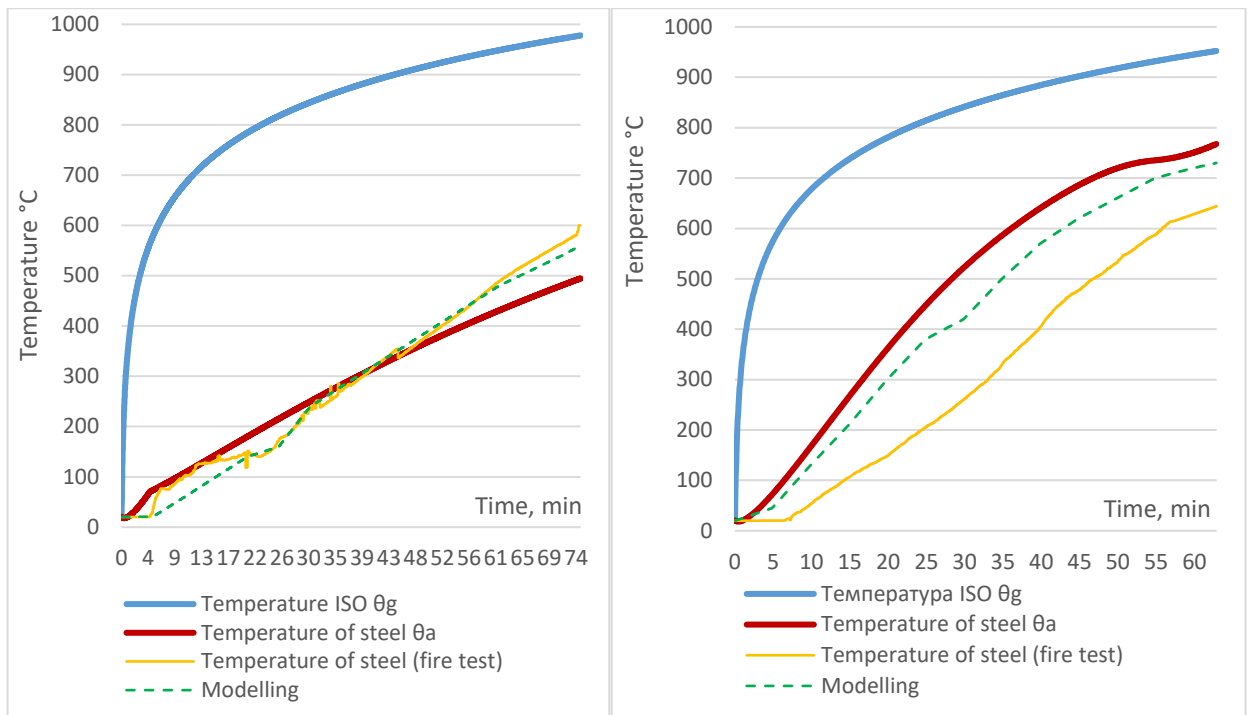
No	Test samples		
1			
2			



**Figure 8. Graphic of temperature changes at thermocouples on protected samples (monitor of test equipment TIZOL JSC).**

Critical deformations of the I-shaped cross section occurred at 74 minutes 27 seconds of testing. The average temperature of the cross section according to the results of thermocouples is 567.7 °C and it is accepted as critical. For the box-shaped section, the critical temperature is 624.5 °C and it reached at 57 minutes 10 seconds. The accuracy of experimental results is ensured by the sufficient number of thermocouples and the experimental error does not exceed 10 %.

The summary table of the solution of the both static, thermophysical problems and results of fire tests are presented in Table 7.



**Figure 9. Fire exposure curves (calculated and actual) for protected samples.**

**Table 7. Data summary on critical temperatures and fire resistance limits for protected samples.**

Calculation method	Sample 1		Sample 2	
	Calculation	Fire test	Calculation	Fire test
Static calculation. Critical temperatures, °C				
Critical temperatures °C	547.27°C	567.7°C	713.08°C	624.5°C
Thermophysical calculations. Fire resistance limits, min				
Analytical solution	86	74:27	49	57:10
Simulation	75		58	

The best convergence to the actual results of fire tests was shown by the simulation in the software package. This is due to the implementation of the air gap in the design model inside the fire protected structure and a comprehensive accounting of changing properties of fire protection. Analytical methods do not take these points into account to simplify the calculation scheme.

#### 4. Conclusions

The paper analyzes the applicability of existing numerical methods for calculating of the fire resistance limits of thin-walled constructions, including those with fire protection. It is shown that when solving the static part of the calculation, the assumption of a critical temperature of 350 °C represents a significant underestimation of the structure's bearing capacity. This result is familiar with the studies [13–18] and shows that some complex structures (like 2xC columns or beams) made of high-strength steel can retain their bearing capacity at temperatures up to 500-600°C at least as normal thick-walled construction.

Validation of the static and thermophysical parts of the fire resistance calculation shows that the solution of the thermophysical problem on the basis of finite element modeling of temperature fields is the most precise method to estimate time of critical deformations in accordance to the criteria of structure heating up to the critical temperature. The most applicable C and  $\Sigma$  cross-sections of building structures with and without fire protection are considered.

The recommendations are given on application of program complexes in solving thermophysical problem of fire resistance calculation.

#### 5. Acknowledgments

The research is partially funded by the Ministry of Science and Higher Education of the Russian Federation as part of World-class Research Center program: Advanced Digital Technologies (contract No. 075-15-2020-934 dated on 17.11.2020)

The authors are grateful for providing the results of the fire experiments to the management of TIZOL JSC, and also thank the specialists of Andrometa LLC for providing technical and informational support in carrying out this work.

#### References

1. Musorina, T.A., Gamayunova, O.S., Petrichenko, M.R., Soloveva, E. Boundary layer of the wall temperature field. *Advances in Intelligent Systems and Computing*. 2020. Vol. 1116. Pp. 429–437.
2. Musorina, T., Gamayunova, O., Petrichenko, M. Thermal regime of enclosing structures in high-rise buildings. *Vestnik MGSU*. 2018. Vol. 13. Pp. 935–943.
3. Dinis, P.B., Camotim, D. Local distortional mode interaction in cold-formed steel lipped channel beams. *Thin-Walled Structures*. 2010. 48. Pp. 771–785.
4. Narayanan, S., Mahendran, M. Ultimate capacity of innovative cold-formed steel columns. *Journal of Constructional Steel Research*. 2003. 59. Pp. 489–508.
5. Pan, C-L, Shan, M-Y. Monotonic shear tests of cold-formed steel wall frames with sheathing. *Thin-Walled Structures*. 2011. 49. Pp. 363–370.
6. Wang, H., Zhang, Y. Experimental and numerical investigation on cold-formed steel C-section flexural members. *Journal of Constructional Steel Research*. 2009. 65. Pp. 1225–1235.
7. Zaharia, R., Dubina, D. Stiffness of joints in bolted connected cold-formed steel trusses. *Journal of Constructional Steel Research*. 2006. 62. Pp. 240–249.
8. Terekh, M., Tretyakova, D. Primary energy consumption for insulating. *E3S Web of Conferences*. 2020. Vol. 157. P. 8.
9. Zemitis, J., Terekh, M. Optimization of the level of thermal insulation of enclosing structures of civil buildings. *MATEC Web of Conferences*. 2018. Vol. 245.
10. Kaitila, O. Imperfection sensitivity analysis of lipped channel column at high temperatures. *Journal of Constructional Steel Research*. 2002. 58. Pp. 333–351.
11. Ranawaka, T., Mahendran, M. Numerical modeling of light gauge cold-formed steel compression members subjected to distortional buckling at elevated temperatures. *Thin-Walled Structures*. 2010. 48, Pp. 334–344.
12. EN 1993-1-2:2005. Eurocode 3. Design of steel structures Part 1-2. General rules. Structural fire design.
13. Kankanamge, N.D., Mahendran, M. Behaviour and design of cold-formed steel beams subject to lateral-torsional buckling at elevated temperatures. *Thin-Walled Structures*. 2012. 61. Pp. 213–228.
14. Kankanamge, N.D. Structural behaviour and design of cold-formed steel beams at elevated temperatures [Ph.D. Thesis]. Brisbane, Australia: Queensland University of Technology; 2010.
15. Laím, L., Rodrigues, J.P.C. Fire behaviour of cold-formed steel beams for industrial buildings. *Proceedings of the 1<sup>st</sup> Ibero-Latin-American congress on fire safety, Natal, Brazil*. 2011. 1. Pp. 53–62.
16. Lu, W., Mäkeläinen, P., Outinen, J. Numerical simulation of catenary action in cold-formed steel sheeting in fire. *Proceedings of the fifth international conference on thin-walled structures*. Brisbane, Australia. 2008. Pp. 713–720.

17. Laím, L., Rodrigues, J.P.C., Simões, D.V. Experimental and numerical analysis on the structural behaviour of cold-formed steel beams. *Thin-Walled Structures*. 2013. 72. Pp. 1–13.
18. Gravit, M., Dmitriev, I. Fire Resistance of Loaded I-Section Column from Light Gauge Steel Thin-Walled Profiles. In: Anatolijs B., Nikolai V., Vitalii S. (eds) *Proceedings of ECECE 2019*. ECECE 2019. Lecture Notes in Civil Engineering. 2020. Vol. 70. Springer, Cham.
19. Vatin, N. et al. Simulation of cold-formed steel beams in global and distortional buckling. *Applied Mechanics and Materials*. 2014. Vol. 633–634. Pp. 1037–1041.
20. Garifullin, M., Nackenhorst, U. Computational analysis of cold-formed steel columns with initial imperfections // *Procedia Engineering*. 2015. Vol. 117. No. 1. Pp. 1073–1079.
21. Garifullin, M. et al. Buckling analysis of cold-formed c-shaped columns with new type of perforation. *Advances and Trends in Engineering Sciences and Technologies – Proceedings of the International Conference on Engineering Sciences and Technologies, ESaT 2015*. 2016. Pp. 63–68.
22. Gravit, M., Dmitriev, I., Lazarev, Y. Validation of the Temperature Gradient Simulation in Steel Structures in SOFiSTiK. *Advances in Intelligent Systems and Computing*. 2019. Vol. 983. Pp. 929–938.
23. Gravit, M.V., Nedryshkin, O.V. Full-scale tests for the simulation of fire hazards in the building with an atrium. *Advances and Trends in Engineering Sciences and Technologies III- Proceedings of the 3<sup>rd</sup> International Conference on Engineering Sciences and Technologies, ESaT 2018*. 2019. Pp. 375–380.
24. Naser, M.Z., Degtyareva, N.V. Temperature-induced instability in cold-formed steel beams with slotted webs subject to shear. *Thin-Walled Struct.* 2019. Vol. 136. Pp. 333–352. DOI: 10.1016/j.tws.2018.12.030
25. Naser, M.Z., Uppala, V.A. Properties and material models for construction materials post exposure to elevated temperatures. *Mech. Mater.* 2020. Vol. 142. DOI: 10.1016/j.mechmat.2019.10329318.
26. Zhou H. et al. Behavior of prestressed stayed steel columns under fire conditions. *Int. J. Steel Struct.* 2017. Vol. 17. No. 1. Pp. 195–204. DOI: 10.1007/s13296-015-0074-4
27. Chen, W. et al. Full-scale experiments of gypsum-sheathed cavity-insulated cold-formed steel walls under different fire conditions. *J. Constr. Steel Res.* Elsevier. 2020. Vol. 164. Pp. 105809. DOI: 10.1016/J.JCSR.2019.105809
28. Chen, W., Ye, J., Zhao, Q. Thermal performance of non-load-bearing cold-formed steel walls under different design fire conditions. *Thin-Walled Struct.* Elsevier. 2019. Vol. 143. Pp. 106242. DOI: 10.1016/J.TWS.2019.106242
29. Chen, W., Ye, J., Li, X. Fire experiments of cold-formed steel non-load-bearing composite assemblies lined with different boards. *J. Constr. Steel Res.* 2019. Vol. 158. Pp. 290–305. DOI: 10.1016/j.jcsr.2019.04.003
30. Chen, W., Ye, J., Li, X. Thermal behavior of gypsum-sheathed cold-formed steel composite assemblies under fire conditions. *J. Constr. Steel Res.* 2018. Vol. 149. Pp. 165–179. DOI: 10.1016/j.jcsr.2018.07.023
31. Chen, W. et al. Improved fire resistant performance of load bearing cold-formed steel interior and exterior wall systems. *Thin-Walled Struct.* Elsevier. 2013. Vol. 73. Pp. 145–157. DOI: 10.1016/J.TWS.2013.07.017
32. Dias, Y., Keerthan, P., Mahendran, M. Fire performance of steel and plasterboard sheathed non-load bearing LSF walls. *Fire Saf. J.* 2019. Vol. 103. Pp. 1–18. DOI: 10.1016/J.FIRESAF.2018.11.005
33. Dias, Y., Mahendran, M., Poologanathan, K. Full-scale fire resistance tests of steel and plasterboard sheathed web-stiffened stud walls. *Thin-Walled Struct.* 2019. Vol. 137. P. 81–93. DOI: 10.1016/j.tws.2018.12.027

### **Contacts:**

*Marina Gravit, marina.gravit@mail.ru*

*Ivan Dmitriev, i.i.dmitriev@yandex.ru*